Higher-order mode analysis of multi-cell axisymmetric superconducting cavities through measurements and numerical calculations

John Popielarski, Leo Kempel

Department of Electrical and Computer Engineering, Michigan State University, East Lansing, Michigan, 48824 USA

Terry Grimm, Walter Hartung, Felix Marti

National Superconducting Cyclotron Laboratory, Michigan State University, East Lansing, Michigan, 48824 USA

Abstract.

Design of superconducting multi-cell cavities and evaluation of their electromagnetic (EM) properties relies heavily on the use of numerical calculations by computer code. Analysis of the cavity's higher-order modes (HOMs) and its associated power couplers are greatly facilitated by computer simulation. Nevertheless, RF measurements are essential to verify numerical predictions. We compare the results of numerical calculations of the EM properties of HOMs to RF measurements on a copper model of a 5-cell superconducting cavity. The EM properties of the fundamental pass-band mode are also compared. The main EM properties of interest are the frequency, shunt impedance and the strength of the coupling to the input coupler. The measurements are done with a bead-pull system and a network analyzer. The multi-cell cavity is being developed for the acceleration of beams traveling of about 0.47 times the speed of light.

1. Introduction

While the use of computer simulation greatly facilitates the design of radio frequency (RF) cavities, it is important to confirm simulations with measurements. This paper compares computer simulation results for a 5-cell axisymmetric copper cavity with RF measurements. The cavity is a prototype of a 6-cell superconducting cavity designed to accelerate beams at about 47% of the speed of light. The 6-cell cavity is being developed for the Rare Isotope Accelerator [1, 2]. Much of the HOM analysis for the 6-cell cavity was done with *MAFIA* [3]. Additional *MAFIA* simulations were done for the 5-cell case for comparison with the measurements.

The beam stability can be predicted from the HOM frequency (f), geometric shunt impedance (R_a/Q_0) and coupling strength (Q_{ext}), which are explained in Section 1.2. The quality factor (Q_0) is also important for the system performance. Because the RF measurements are done on a room temperature copper model of the cavity, its Q_0 is much lower than an actual superconducting niobium cavity. Therefore, a room temperature measurement of Q_0 is not very useful. All of the other quantities were calculated numerically and measured.

The field profile is measured via a "bead pull" perturbation method in order to calculate R_a/Q_0. The field profile is also used to evaluate the field flatness of the cavity.

1.1. Multi-cell Cavity and HOMs

Figure 1 shows a multi-cell cavity, with a coaxial power coupler. Aside from the coupling ports, the cavity is axisymmetric about the beam axis. The modes in the elliptical cells are classified by analogy to the modes in an ideal pillbox (TM_{mnp} and TE_{mnp} where the subscripts mnp refer to the azimuthal, radial and longitudinal variations). In general, elliptical cavity modes are not necessarily pure transverse magnetic (TM) or transverse electric (TE), although they are more like one or the other. One mode of a single cell cavity splits into 5 pass-band modes in a five cell cavity. Additionally, multi-pole modes have two different polarizations which split in frequency due to asymmetries. Two modes of a five-cell cavity are shown in Figure 3 below.

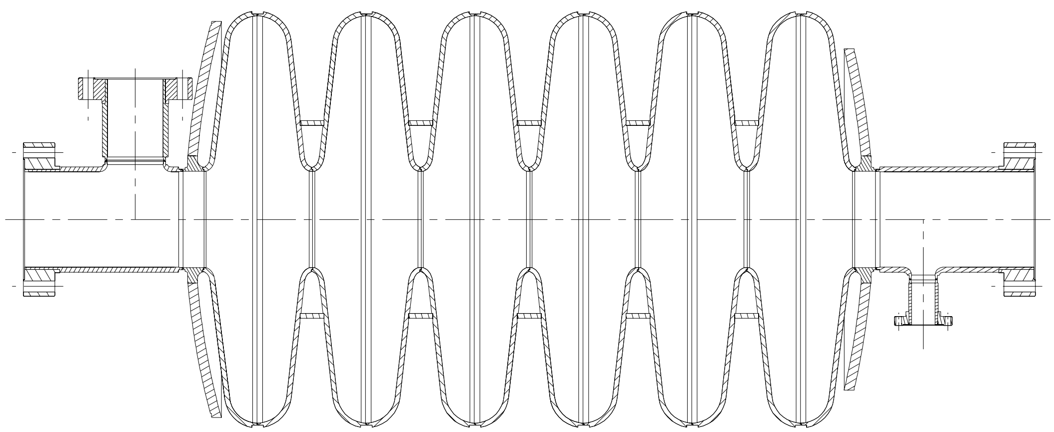

Figure 1. Six-cell axisymmetric cavity with power coupler port on the left.

1.2. Some important HOM quantities

Some important HOM properties that are obtained through computational means can also be obtained through bench-top measurements. Quantities that are independent of the cavity material are most desirable. There are other important quantities for cavity design, including peak electric and magnetic fields, but they are not easily measured.

The shunt impedance and quality factor of the superconducting cavity are two important figures of merit. Both of these depend on the surface resistance of the cavity walls. Dividing the shunt impedance by the quality factor gives a useful material-independent quantity (R_a/Q_0). The R_a/Q_0 of a cavity mode is an integral of the longitudinal electric field (E_z). For TM monopole modes, E_z exists along the beam axis, where the other electric and magnetic field components are very small. For all other modes, E_z goes to zero along the beam axis. Since beam instabilities [4] can occur due to any mode with non-zero E_z on or near the axis, it is important to calculate R_a/Q_0 for modes other than the accelerating mode.

The coupling strength of the power coupler is determined from the external quality factor (Q_{ext}). The Q_{ext} of the accelerating mode must be small enough to accommodate the beam loading of the accelerating mode; the Q_{ext} of the HOMs determine the rate of damping of beam induced fields in the HOMs and hence the beam stability. The Q_{ext} calculations for multi-cell cavities can be difficult because simulations require large mesh sizes due the to larger structure and the asymmetric geometry. However, a 3D code can be used to calculate the single cell Q_{ext} for each mode. Multi-cell modes can be more easily calculated with 2D meshes; the 2D calculation give an energy ratio (the ratio of the total stored energy to the energy in the cell adjacent to the coupler). Multiplying the Q_{ext} of the single cell cavity mode by the energy ratio for each multi-cell mode in the multi-cell pass-band provides an adequate approximation of the multi-cell Q_{ext} values. If all of the cells have the same energy, the 6-cell Q_{ext} is 6 times the single cell Q_{ext}. This method requires a knowledge of which single cell mode corresponds to each multi-cell passband. This can be determined by viewing graphical simulation results, but it is not always straightforward.

1.3. Computer Simulations

MAFIA [3] and *ANALYST* [5] were used for numerical calculation of cavity eigenmodes. Simulations where done on simple 5-cell (no power coupler) axisymmetric geometries in 2D. Necessary 3D simulations, such as the design of the power coupler, were done with a single-cell geometry.

1.4. Measurements

The measurements were done with a vector network analyzer (VNA) and a bead pull mechanism, as shown in Figure 2. Simple wire antennae of different shapes and sizes were used to couple to different modes. The antennae were mounted on the beam tube end-caps. The Q_{ext} was measured in transmission.

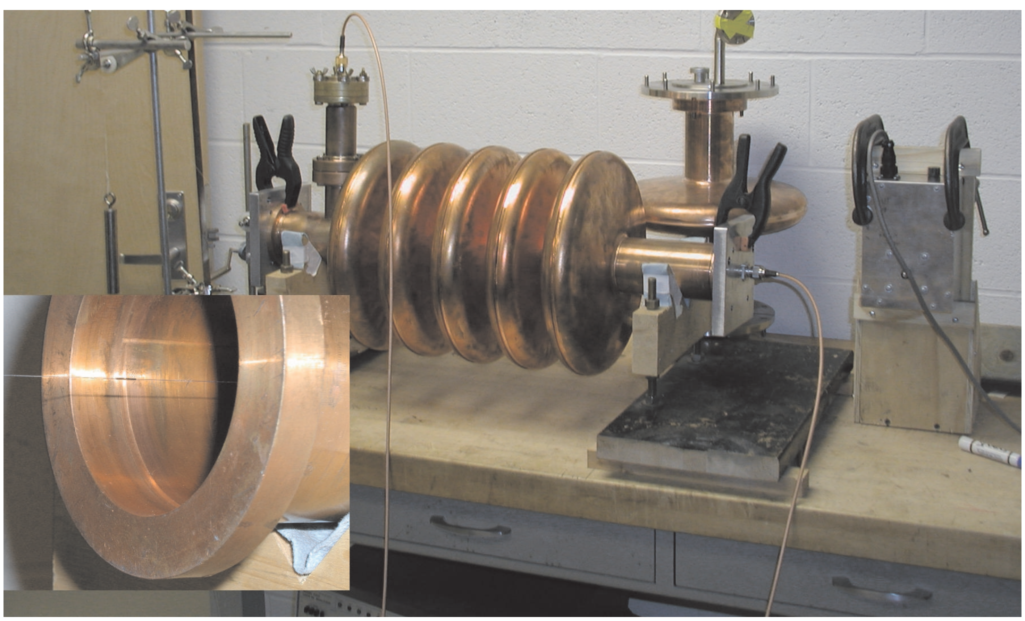

Figure 2. Set-up for bead-pull measurements. The input antenna is mounted onto the right end-cap. The power coupler on the left beam tube may be used as a pickup, although an additional antenna on the left end-cap was used in some cases. The inset shows the metallic needle and the fishing line (controlled by the motor on the right). The Q_{ext} is measured with the same set-up, adjusting the input antenna for unity coupling.

2. Theory

MAFIA can calculate the relevant mode properties directly from their theoretical definitions. For measurement, manipulation of the theoretical definitions is needed in order to relate the mode properties to the S-Parameters that can be measured with a network analyzer.

2.1. Definitions

The quality factor of the cavity is the ratio of the stored energy in the cavity times the angular frequency to the power dissipated in the cavity walls. The power dissipated, P_c, is dependent on the surface resistance, R_s, of the cavity walls. The shunt impedance is determined from the average voltage seen by the beam, V_c, and the dissipated power, P_c. The beam voltage is calculated from the longitudinal electric field along the beam axis $(a = 0)$, for monopole modes, or near the beam axis $(a \neq 0)$ for multi-pole modes:

$$V_c = \left| \int_0^d E_z(\rho = a, z) \exp\left(\frac{i\omega_0 z}{c\beta} \right) dz \right|, \tag{1}$$

where ω_o is the resonant angular frequency of the mode, $c\beta$ is the velocity of the beam, d is the total length of the cavity, and ρ is the radial cylindrical coordinate. Thus, V_c is the integral of the longitudinal force on a particle traveling at the speed $c\beta$, accounting for the time and space dependence in the field, with the particle traveling on the crest of the wave. The shunt impedance (linac definition) is

$$R_a = \frac{V_c^2}{P_c}. \tag{2}$$

The external quality factor, Q_{ext}, is a ratio of the stored energy times ω_o to the power emitted out of the power coupler. If other losses are assumed to be small, the overall Q of the cavity, the loaded Q, (Q_L), can be expressed in terms of Q_0 and Q_{ext} only; it is measured with the VNA from the bandwidth of the resonance. Typically, operational values of Q_{ext} are very large for superconducting cavities, i.e. the coupling is weak. The Q_{ext} can be determined from Q_L via a measurement of the transmission coefficient (S_{21}). With unity coupling (matched load),

$$Q_{ext} = \frac{2\,Q_L}{|S_{21}|^2} \tag{3}$$

If the input antenna does not have unity coupling, a correction factor may be determined from the reflection coefficient (S_{11}). It is preferred to be near unity coupling in order to minimize systematic errors in the measurement.

2.2. Perturbation by a metallic object

Using Slater's perturbation theory, it is possible to calculate the normalized field strength, $\vec{E}_o$ and/or $\vec{H}_o$, by introducing a small metallic perturbation and measuring the change in resonant frequency. A metallic sphere may be used to determine E_z along the beam axis for all TM monopoles, because for these modes the other field components are very small.

For other modes, a metallic needle can be used in combination with a calibration constant. This constant may be derived theoretically [6, 7] or determined experimentally. The metallic needle changes the resonant frequency significantly due only to the presence of an electric field, and the frequency change is greatest when the needle is oriented in the direction of the electric field [7]. With a small change in resonant frequency, $\Delta\omega \ll \omega_o$, Slater's perturbation can be approximated for a sphere by:

$$\Delta\omega = 4\pi\omega_o a^3 \left(\varepsilon \vec{E_o}^2 - \frac{1}{2}\mu \vec{H_o}^2 \right) \tag{4}$$

where $\vec{E_o}^2$ and $\vec{H_o}^2$ are normalized by dividing by twice the cavity's stored energy and a is the radius of the sphere. The technique used herein is a simple method to quickly measure the R_a/Q_0 of a particular mode and compare with *MAFIA*. Therefore, it is only desired to measure the z-component of the electric field on or near the beam axis. A needle was used with calibration through a $TM_{010,\pi}$ measurement with a sphere.

Sphere. For TM monopole modes, E_z is the only field component along the axis, which simplifies Equation (4). The R_a/Q_0 for TM monopoles can be calculated numerically from

$$\frac{R_a}{Q_0} = \frac{\left| \int \sqrt[\pm]{\Delta\omega} \exp\left(\frac{i\omega_o z}{c\beta}\right) dz \right|^2}{4\pi\varepsilon_o \omega_o^2 a^3}, \tag{5}$$

allowing us to obtain R_a/Q_0 for a given β from the bead-pull measurement of $\Delta\omega$ as a function of z.

Needle. A needle was also used, (see Figure 2) to evaluate E_z. Multi-pole modes are measured by moving off axis 2 cm in the direction corresponding to the strongest coupling: R_a/Q_0 can be determined for any $(\rho,\, \phi)$ coordinate. This is done by coupling to the mode with an off-axis antenna and doing the bead-pull 2 cm off axis and 180° in rotation from the antenna. The two polarizations of the HOMs are measured by rotating the antenna and bead until that the other polarization is coupled (at a different frequency). With a needle of volume $\pi a^2 l$,

$$\frac{R_a}{Q_0} = k \frac{\left| \int \sqrt[\pm]{\Delta\omega} \exp\left(\frac{i\omega_o z}{c\beta}\right) dz \right|^2}{4\pi\varepsilon_o \omega_o^2 a^2\, l} \tag{6}$$

The proportionality constant k in Equation (6) may be determined experimentally from either a known cavity, such as a pillbox, or from a monopole mode measurement. The R_a/Q_0 results in this paper were obtained from needle measurements, using a proportionality constant obtained from the $TM_{010,\pi}$ mode with the sphere as a calibration standard.

3. Calculation, measurement procedures and results

3.1. Field profiles and R_a/Q_0

MAFIA was used to calculate the E_z profiles on or near the beam axis for all relevant HOMs [1]. Figure 3 compares two *MAFIA* profiles with the measured profiles. The mode classification is determined from the field distribution, a step which is also required to predict the multi-cell Q_{ext}, as explained in Section 1.1.

Figures 3a and 3b show the raw data collected: the S_{21} phase shift ($\Delta\phi$) as a function of bead position. The bead position is determined by measuring the distance and time of the bead travel. The S_{21} phase shift is proportional to the change in resonant frequency due to the perturbation. The frequency change is calculated from the phase shift by interpolating a measurement of phase as a function of frequency for the unperturbed cavity mode. Using

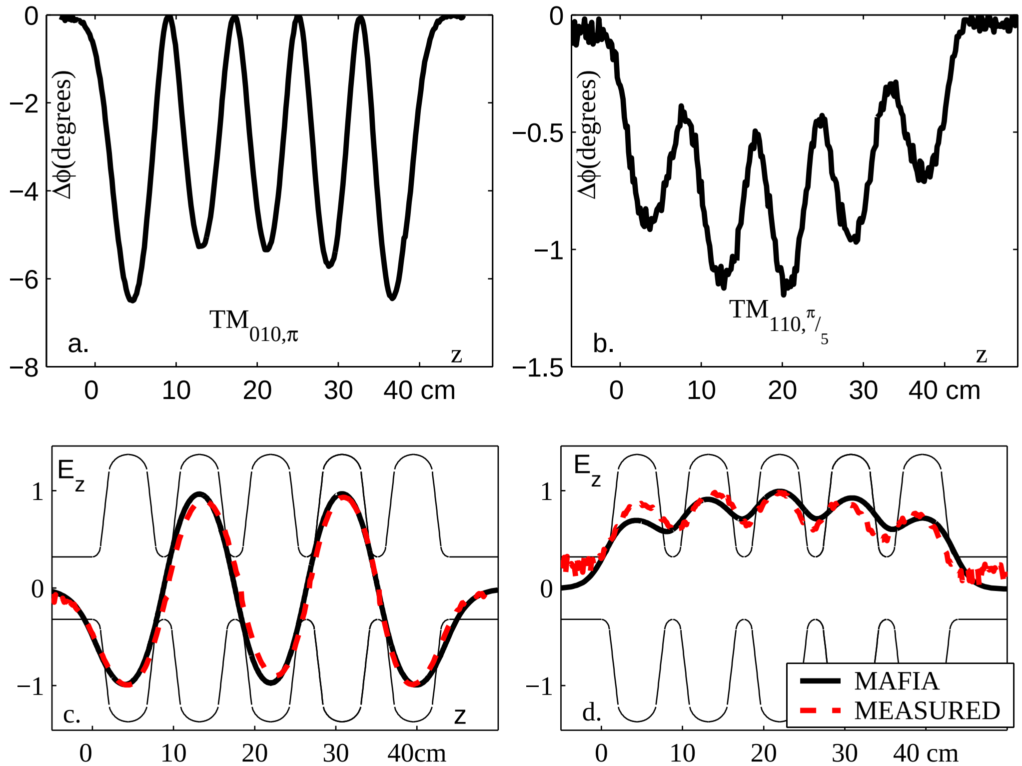

Figure 3. (a) Raw data collected for the accelerating mode along the beam axis from a metallic needle perturbation. (b) Data collected for a dipole mode 2 cm off axis. (c,d) Comparison of normalized E_z profiles, taken from the measurements in (a,b).

a conducting needle (radius = 0.25mm, length = 6.34 mm), the maximum $\Delta\phi$ was about 7° for the $TM_{010,\pi}$ mode (Figure 3a), which corresponds to 3.00 kHz change in frequency. For the $TM_{010,\pi/5}$ mode (Figure 3b), the conducting needle was placed off-axis 2 cm, and the maximum phase change was only about 1.2°, corresponding to a Δf_{max} of 574 Hz. Figures 3c and 3d show a comparison of *MAFIA* to the measurements. Prior measurements were done with the conducting sphere, and the calibration constant k was determined to be 1.15 from the monopole measurement. Data manipulation is needed to account for a change in the direction of the E_z field (e.g. the field changes direction four times in Figure 3c) and then R_a/Q_0 can be numerically calculated from Equation (6) with the calibration constant. The results are shown in Table 1.

The cavity is designed to accelerate the beam from $\beta = 0.40$ to $\beta = 0.52$, where βc is the beam velocity. Hence, the dependence of R_a/Q_0 on β is of interest. Figure 4a shows the dependence of the measured R_a/Q_0 on β, as obtained via Equation (5). *MAFIA* was also used to calculate the dependence on β via Equations (1) and (2) and the results are shown in Figure 4b. The maximum R_a/Q_0 was used when evaluating beam stability issues [1]. Because the locations of the zeros rely heavily on exact bead displacement measurements, measuring the maximum R_a/Q_0 over the range of interest gives better agreement without a complicated set-up.

Table 1. Summary of measured and simulated frequencies and shunt impedances. The listed R_a/Q_0 values are the maximum values in the range $0.40 \leq \beta \leq 0.52$. The dipole modes were evaluated at a radius of 2 cm.

Mode	**Frequency (MHz)**		R_a/Q_o **(Ω)**	
	Simulated	***Measured***	***Simulated***	***Measured***
$TM_{010,\pi/5}$	794.0	794.4	.0652	.0431
$TM_{010,2\pi/5}$	797.0	797.7	.268	.515
$TM_{010,3\pi/5}$	800.6	801.5	3.94	3.28
$TM_{010,4\pi/5}$	803.5	804.7	37.8	25.6
$TM_{010,\pi}$	804.7	805.8	162.2	156.4
$TM_{110,\pi}$	1133	1132	6.744	3.984
$TM_{110,4\pi/5}$	1139	1140	13.095	26.47
$TM_{110,3\pi/5}$	1147	1149	7.130	5.202
$TM_{110,2\pi/5}$	1156	1158	3.534	5.577
$TM_{110,\pi/5}$	1161	1164	.8562	1.542

3.2. Coupling measurements

The measurement of Q_{ext} is done on the accelerating mode in order to design the input coupler. The Q_{ext} can be calculated from Equation (3) and measurements of Q_L and the *S*-Parameters. The VNA is connected to the power coupler and an antenna in the beam tube. The antenna is constructed such that it is close to a matched load.

Calculation of Q_{ext} for a single cell cavity was done in [1] using *ANALYST*. *MAFIA* could also be used to compute Q_{ext} using the procedure in [8]. The multi-cell Q_{ext} was computed from 2D *MAFIA* simulations. The predicted Q_{ext} for some HOMs are presented in Table 2.

4. Discussion

The measured results in Tables 1 and 2 provide good agreement with the simulated results for the fundamental pass-band. However, there are significant discrepancies in R_a/Q_0 at certain velocities. The Q_{ext} measurements are in good agreement for the multi-cell pass-band modes and single cell modes, while HOM dipoles do have a discrepancy.

The R_a/Q_0 measurements were all done with a calibrated needle, although measurements with a conducting sphere should provide accurate results for monopole modes.

The measured Q_{ext} values were generally lower than the simulated values. The energy distribution could be affected by the input coupler. This could, in effect, lower the expected energy ratio as simulated in the ideal case with *MAFIA*. The measured profiles of the HOMs evaluated without the penetrating input coupler did have good agreement, corresponding to an energy ratio agreement in the vicinity of $\pm 10\%$. The energy ratios in the presence of the penetrating input coupler were not evaluated.

Several modes were simulated for the 6-cell cavity [1]. All the monopole, dipole, quadrupole, and sextupole modes below their cut-off frequencies (both TM and TE) were simulated using an axisymmetric geometry. The R_a/Q_0, energy ratios, single-cell Q_{ext} and frequencies were all considered to identify possible problematic modes.

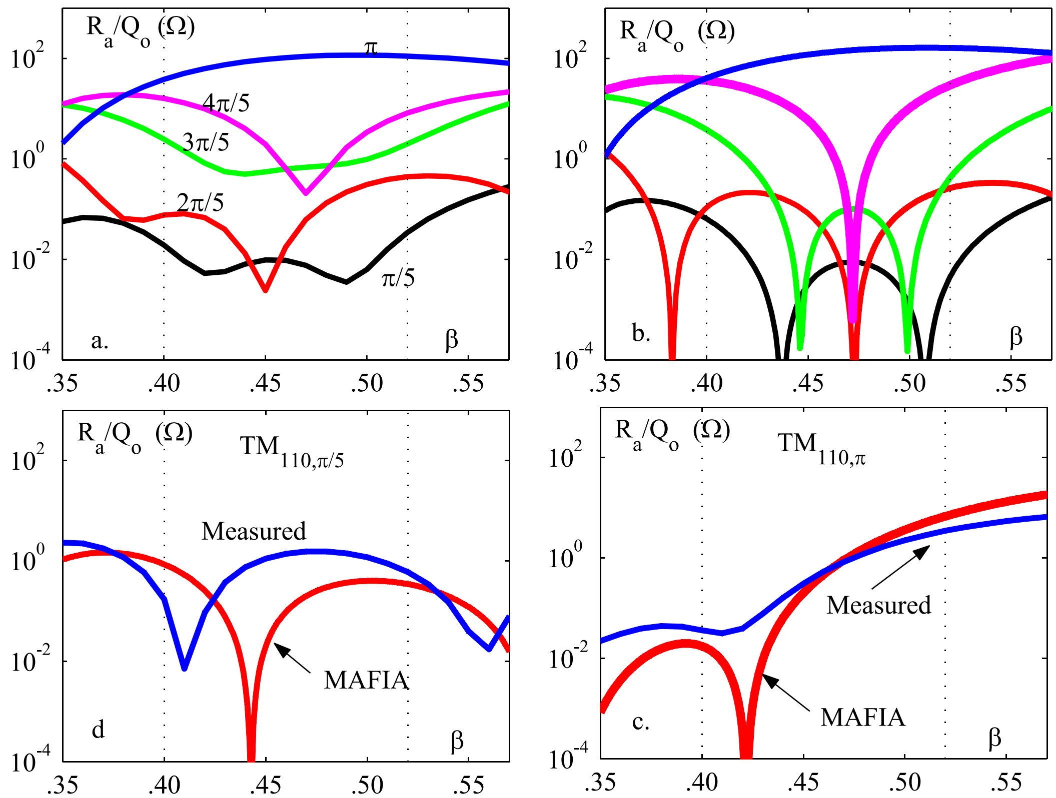

Figure 4. The measured (a) and simulated (b) R_a/Q_0 as a function of beam velocity for the fundamental passband. The figures illustrate the misalignment of the measured data due to inaccurate displacement measurements, which can lead to large disagreement with the simulation results for certain discrete points. Graphs (c) and (d) compare two modes in the the TM_{110} pass-band.

5. Conclusion

Simple RF measurements were done on a copper model of a superconducting cavity at room temperature to confirm some key RF properties. Though the results presented in this paper provide reasonable agreement with the simulation results, more accurate measurements are possible, although this would require additional equipment and more complicated set-ups.

The measurements of the field profile could be improved with an automated system, such a PC connected to the VNA and an electronic displacement sensor, simultaneously taking measurements. Additionally, the path of the bead should be parallel to the beam axis. The bead can deviate from this path if the guides on the ends of the cavity are not properly aligned.

The computer simulations provided accurate results and were a great facilitator in the development of the 6-cell cavity, and the RF measurements provided a good confirmation of the simulations.

Acknowledgments

We thank the entire SRF group at NSCL, especially Steve Cossmann, Holger Podlech, Roger Zink and Richard York. This work is supported by the US Department of Energy under grant

Table 2. Summary of measured and simulated coupling strengths. The energy ratio is of the total energy to the energy in the end cell. The simulated 5-cell Q_{ext} values were calculated by multiplying the simulated energy ratios by the simulated Q_{ext}.

	Frequency (MHz)		Ratio	$Q_{ext,5-cell}$	
Mode	***Simulated***	***Measured***	***Simulated***	***Simulated***	***Measured***
$TM_{010,single}$	805.0	799.7	–	2.170×10^6	2.820×10^6
$TM_{010,\pi/5}$	794.0	794.4	23.75	5.154×10^7	3.116×10^7
$TM_{010,2\pi/5}$	797.0	797.7	6.817	1.479×10^7	1.040×10^7
$TM_{010,3\pi/5}$	800.6	801.5	3.744	8.124×10^6	6.266×10^6
$TM_{010,4\pi/5}$	803.5	804.7	2.839	6.161×10^6	4.480×10^6
$TM_{010,\pi}$	804.7	805.8	5.319	1.115×10^7	6.380×10^6
$TM_{020,single}$	1725	1725	–	3.410×10^5	4.420×10^5
$TM_{020,\pi/5}$	1702	1703	10.93	3.727×10^6	2.773×10^6
$TM_{020,2\pi/5}$	1712	1713	3.828	1.305×10^6	3.816×10^5
$TM_{020,3\pi/5}$	1726	1728	3.055	1.042×10^6	2.805×10^5
$TM_{020,4\pi/5}$	1741	1743	4.280	1.459×10^6	3.579×10^5
$TM_{020,\pi}$	1752	1754	13.17	4.491×10^6	1.250×10^6
$TM_{110,1cell}$	1154.70	1149.5	–	9.580×10^5	1.090×10^6

DE-FG02-00ER41144. The elliptical cavity development at NSCL is being carried out in collaboration with Thomas Jefferson National Laboratory and INFN-Milano.

References

[1] Grimm T, Hartung W, Marti F, Podlech H, York R C, Popielarski J, Wiess C, Kempel L, Ciovati G, Kneisel P 2002 Input Coupling and Higher-Order Mode Analysis of Superconducting Cavities for the Rare Isotope Accelerator in Proceedings of the Eight European Particle Accelerator Conference (Geneva: EPS-1GA Publishing) p. 2241

[2] Compton C C, Grimm T L, Hartung W, Podlech H, York R C, Ciovati G, Kneisel P, Barni D, Pagani C, Pierini P 2001 Niobium Development for the High-Energy Linac of the Rare Isotope Accelerator in Proceedings of the 2001 Particle Accelerator Conference (Piscataway, New Jersey: IEEE Publishing) p. 1044

[3] Mafia 4, Computer Simulation Technology, Darmstadt, Germany (http://www.cst.de)

[4] Padamsee H, Knobloch J and Hays T 1998 RF Superconductivity for Accelerators (New York: John Wiley & Sons, Inc.) p 154

[5] Analyst, Simulation Technology & Applied Research, Inc., Wisconsin, USA (http://www.staarinc.com)

[6] Maier L C and Slater J C Field Strength Measurements in Resonant Cavities 1952, Journal of Applied Physics, Vol 23, p 68-77

[7] Ginzton E L 1957 Microwave Measurements (New York: McGraw-Hill) p 446

[8] Balleyguier P 1998 External Q Studies for APT SC-Cavity Couplers in Proceedings of the XIX International Linac Conference (Argonne, Illinois: ANL-98128) p. 133